

IDENTIFICATION OF BIOLOGICAL AEROSOLS BY ITS FLUORESCENCE SPECTRA AND COMPARISON WITH VOLUMETRIC DATA

Egor A. Illarionov^{1,2*}, Svetlana V. Polevova³, Oleg S. Panin¹, Anastasiya A. Konstatinidi¹, Elena E. Severova^{3*}

¹Moscow State University, Department of Mechanics and Mathematics, Leninskiye Gory 1, Moscow, 119991, Russia

²Moscow Center of Fundamental and Applied Mathematics, Leninskiye Gory 1, Moscow, 119991, Russia

³Moscow State University, Department of Biology, Leninskiye Gory 1, Moscow, 119991, Russia

*Corresponding author: egor.illarionov@math.msu.ru, elena.severova@mail.ru

Received: May 20th 2025 / Accepted: January 12th 2025 / Published: March 31st 2026

<https://doi.org/10.24057/2071-9388-2026-4053>

ABSTRACT. An automatic bioaerosol classification system is an attractive alternative to the standard visual identification and counting of pollen in the standard volumetric method of aerobiological monitoring. While various physical principles can be used for automatic measurement of the parameters of particles present in the air, the key problem becomes the development of a classification model based on these data. In particular, practical application of the models becomes challenging due to the large variability of particles present in real air compared to laboratory experiments in which models are usually trained. Instead of training the model on data obtained in laboratory conditions, we applied a clustering algorithm to fluorescence spectra collected during daily measurements in the 2024 season with the Rapid-E+ automatic detector installed at the monitoring station at Moscow State University. Comparison of the temporal distribution of particles in each cluster with the seasonal dynamics of eleven pollen types obtained from standard aerobiological monitoring with a volumetric trap at the same station at Moscow State University shows that some clusters (i.e., fluorescence spectra of specific shape and amplitude) demonstrate temporal patterns similar to pollen seasons. However, the fluorescence spectra alone are not sufficient for differentiation of individual pollen types, and they can only provide detection of larger groups of bioaerosols. Interestingly, the detected larger groups show more diverse seasonal patterns than those observed by volumetric monitoring at the station at Moscow State University. This result demonstrates that automatic detectors can provide more useful information on the content and seasonal distribution of bioaerosols compared to standard volumetric methods.

KEYWORDS: bioaerosol classification, cluster analysis, automatic detector, pollen

CITATION: Illarionov E. A., Polevova S. V., Panin O. S., Konstatinidi A. A., Severova E. E. (2026). Identification Of Biological Aerosols By Its Fluorescence Spectra And Comparison With Volumetric Data. *Geography, Environment, Sustainability*, 1 (19), 29-35

<https://doi.org/10.24057/2071-9388-2026-4053>

ACKNOWLEDGEMENTS: The study was conducted under the state assignment of Lomonosov Moscow State University. It acknowledges the Lomonosov-2 supercomputer center at MSU for providing computational resources and support of the Moscow Center of Fundamental and Applied Mathematics of Lomonosov Moscow State University under agreement No. 075-15-2025-345.

Conflict of interests: The authors reported no potential conflict of interests.

INTRODUCTION

Plant pollen and spores are the main components of biological aerosols and, simultaneously, one of the leading causes of allergic diseases (pollinosis) (Valenta et al. 1992; D'Amato 2000; Sofiev, Bergman 2012; Fröhlich-Nowoisky et al. 2016; D'Amato et al. 2017). Allergies reduce the quality of life for approximately 25–30% of the global population (Dykewicz & Hamilos 2010, Akdis et al. 2015). An essential element of the complex of anti-allergic measures is aerobiological monitoring, which makes it possible to track and predict the dynamics of the concentration of the main allergens in the atmosphere to adjust the therapy and lifestyle of patients with pollinosis.

Currently, the “gold standard” of pollen monitoring is the volumetric pollen trap used for detection and counting

of pollen (Hirst 1952, Galán et al. 2014, Sikoparija et al. 2017, Buters et al. 2018), but these devices are not able to analyze the composition of aerosols in real time. Volumetric samples are identified by a microscopic analysis, which is time-consuming, demands specialized expertise, and involves considerable uncertainties (Šaulienė et al. 2019, Oteros et al. 2017). These problems can be solved with automated aerosol composition analyzers (see An et al. 2024, Kabir et al. 2020, Maya-Manzano et al. 2020, and Huffman et al. 2019, for review of recent progress in different detection techniques), one of which (Rapid E+, Plair, Switzerland) was purchased under the Moscow State University development program and installed in early 2022. In this instrument, the technology for measuring the characteristics of particles in the air stream is based on a combination of light scattering for determination of particle morphology, size,

and velocity, and fluorescence spectroscopy for analysis of fluorescence spectra.

Recently, Erb et al. (2024), Brdar et al. (2023), Boldeanu et al. (2022), Šikoparija et al. (2022), Crouzy et al. (2020), Šaulienė et al. (2019) demonstrated that machine learning models trained on fluorescence spectra combined with other measured pollen parameters can differentiate pollen types. However, these results were obtained in laboratory conditions when the collected pollen of different taxa was injected into the detector. The authors of these models note that adaptation of the models to detection of the learned pollen types in real outdoor conditions meets significant difficulties. The key problem is that a model trained to distinguish pollen of a specific type, such as type A, from another specific type, such as type B, becomes ambiguous when applied to real-world data that includes type A, type B, and a various other pollen types. A practically usable model should be able to distinguish pollen of type A from all other particles present in the air (referred to background particles). However, preparing a corresponding dataset with examples of all other possible particles is unfeasible. As a workaround, for example, Matavulj et al. (2025) proposed to use data collected during the no-pollen season as examples of background particles. However, this approach still cannot capture the full variability of background particles in the pollen season.

Another problem noted in Matavulj et al. (2022, 2025) is that the measurements between different detectors (of the same type) are weakly consistent. Thus, models trained on data from one detector cannot be directly applied to data from another without additional adaptation.

Instead of direct training of classification models, Swanson & Huffman (2020) and Daunys et al. (2021) proposed usage of clustering techniques that help to avoid the problem of collection of the training dataset but require identification of the obtained clusters with specific pollen types.

In this work, we apply a clustering algorithm to fluorescence spectra measured by the automatic atmospheric particle detector Rapid-E+ (which is different from the fluorescence detector used in Swanson & Huffman, 2020) during the 2024 season, and we compare the temporal distribution of particles in each cluster with the temporal distribution of pollen types obtained from daily monitoring with a standard volumetric trap (which extends the approach proposed in Daunys et al., 2021).

MATERIALS AND METHODS

Sampling Campaign

Data for this study were collected from March through October 2024 at the monitoring station at Moscow State

University (Moscow, Russia) using two different sampling campaigns conducted in parallel. In the first campaign, data was collected using the automatic aerosol detector Rapid E+ installed on the roof of one of the buildings on Moscow State University's territory. This device measures various particle parameters based on the physical effects of light scattering and fluorescence, among which we consider only particle size and fluorescence spectrum. It is important to note that by design the automatic detector cannot analyze all particles present in a given volume of flowed air, but only a certain number of them. Moreover, the device measures particles of all types uniformly and cannot prioritize the measurement of one type of particle (e.g., pollen) and ignore other types. To filter out only particles that could potentially include pollen, we apply threshold filtering and select particles with a size larger than $2\mu\text{m}$ and a mean fluorescence intensity above 4000 (this value is also recommended by the manufacturer for pollen analysis). Fig. 1 shows the daily number of particles meeting these criteria during the 2024 season. Due to technical reasons, the device was turned off in June and early July, as well as in mid-August (these periods correspond to zero values in Fig. 1).

In the second campaign, parallel to the automatic detector, data was collected using a Hirst-type volumetric pollen and spore trap (Lanzoni VSSP 2010, Italy) located at the same place as the automated detector. We focused on eleven pollen types (*Acer*, *Alnus*, *Betula*, *Corylus*, *Pinus*, *Poaceae*, *Populus*, *Quercus*, *Salix*, *Ulmus*, *Urtica*). Fig. 2 shows the number of these pollen types and the total amount of detected pollen.

In addition to the above daily measurements, samples of pure pollen from *Betula*, *Quercus*, and *Phleum* were collected from the plants during their pollen periods. Using these examples of pollen, we conducted a laboratory experiment in which the automatic aerosol detector Rapid E+ was placed indoors, and these particles and mixtures of these particles were injected into the device. In more detail, we injected first clean pollen of *Betula*, then *Quercus*, then the mixture of *Betula* and *Quercus* with mass ratio 1:1, then the mixture of *Betula* and *Quercus* with mass ratio 1:3, then clean pollen of *Phleum*, then the mixture of *Betula* and *Phleum* with mass ratio 1:1, then the mixture of *Betula*, *Quercus*, and *Phleum* with mass ratio 1:3:2 correspondingly. Fig. 3 shows the total number of particles detected by the Rapid-E+ per minute, and vertical lines indicate the time moments when the next portions of pollen were injected.

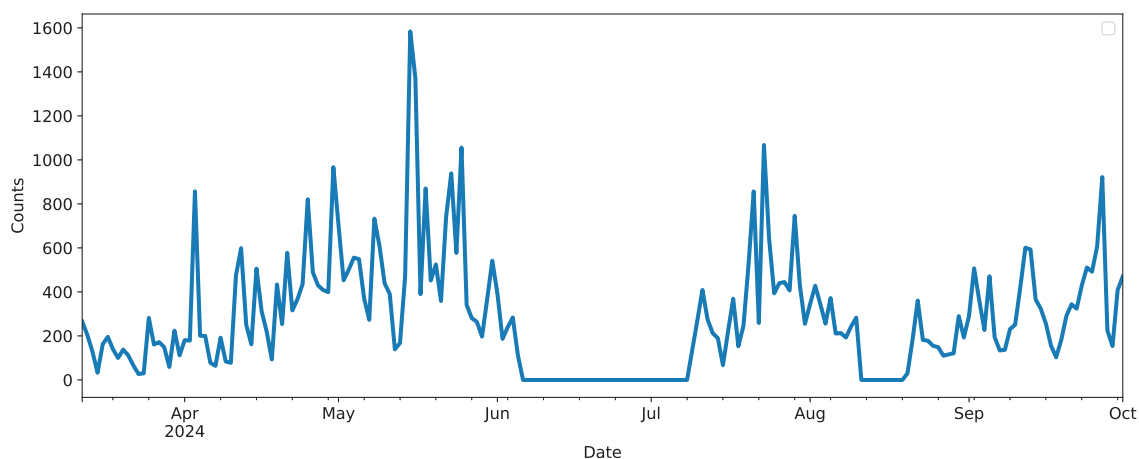


Fig. 1. Number of particles (with size $> 2\mu\text{m}$ and fluorescence threshold > 4000) detected by the automatic detector at the monitoring station at Moscow State University during the 2024 season (zero values mean that the device was turned off)



Fig. 2. Daily counts of different pollen types obtained using the Hirst volumetric method at the monitoring station at Moscow State University during the 2024 season (ALNU - *Alnus*, CORY - *Corylus*, POPU - *Populus*, BETU - *Betula*, QUER - *Quercus*, SALI - *Salix*, ULMU - *Ulmus*, ACER - *Acer*, PINU - *Pinus*, URTI - *Urtica*, POAC - *Poaceae*)

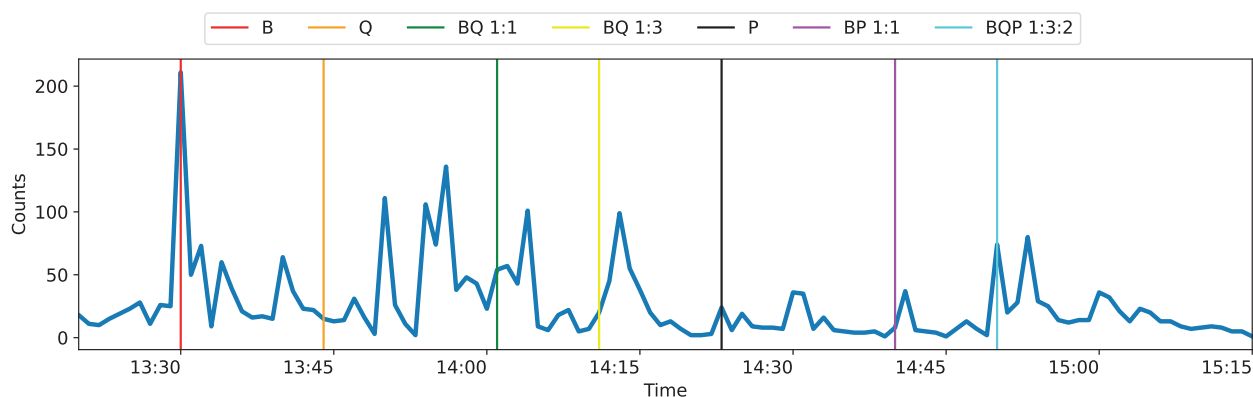


Fig. 3. Particle counts (blue line) during the laboratory experiment. Vertical lines indicate time moments when the new portion of pollen was injected (B is for *Betula*, Q is for *Quercus*, P is for *Phleum*, BQ 1:1 and the similar notations mean the mixture of B and Q with mass ratio 1:1)

Methods

We aim to isolate specific groups of fluorescence spectra within the entire dataset of measured spectra and associate them with particular pollen types using daily monitoring data. The fluorescence spectrum of each particle is given by 16 values representing fluorescence intensity measured at 16 different wavelengths. Particles of different types yield different shapes and amplitudes of the fluorescence spectra. Three different samples shown in Fig. 4 illustrate the variability of the spectra. We observe in Fig. 4 that the spectrum of particle 1 is middle-peaked and strongly non-symmetric; the spectrum of particle 2 is middle-peaked but rather symmetric; and the peak of the spectrum of particle 3 is shifted to the right. Also, amplitudes of the spectra of particles 1 and 3 are much higher than for particle 2. The observed difference in shape and amplitudes motivates us to apply a clustering method for the isolation of different types of spectra.

To divide all measured spectra into subgroups (clusters) containing spectra of similar shape and amplitude, we apply the K -means clustering algorithm (see, e.g., Bishop, 2007). Specifically, each measured spectrum is considered a point in a 16-dimensional space. The goal of the K -means algorithm is to place K new points, considered as cluster centers, in this space in such a way as to minimize the sum of squares of the distance from each point to the nearest center. The number of clusters, K , is set by the user, and the distance is the Euclidean distance. The algorithm finds the optimal location of cluster centers iteratively, starting from some arbitrary positions. Once the method has converged,

each point is assigned to the cluster with the nearest center. The number of clusters, K , is adjusted manually to obtain representative results. It turned out to be useful to isolate a larger number of clusters (compared to the potential number of pollen types) and then merge some clusters that have similar spectrum shapes (but possibly different amplitudes) and similar seasonal patterns.

The final step is to associate each cluster with a specific pollen type. Similar to Fig. 2, we plot daily counts of particles from a given cluster and compare this plot with corresponding plots arising from daily monitoring of known pollen types. If a similar seasonal pattern is found with any known pollen type, then the cluster is identified with that pollen type.

RESULTS

Laboratory experiment

We start with a demonstration of clusters obtained in the laboratory experiment described above (see Fig. 3). To identify clusters corresponding to *Betula*, *Quercus*, and *Phleum*, the K -means clustering algorithm was applied with the number of clusters $K=10$, and the obtained clusters are shown in Fig. 5. The red line in Fig. 5 shows the averaged spectra or cluster center in terms of the K -means algorithm. Some clusters have similar shapes but different amplitudes, for example, clusters 1 and 10 or clusters 2 and 4. One can assume that they represent the same pollen type.

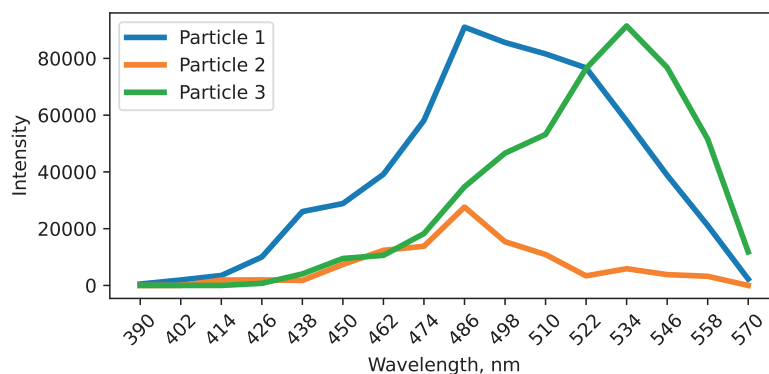


Fig. 4. Examples of fluorescence spectra for three different particles

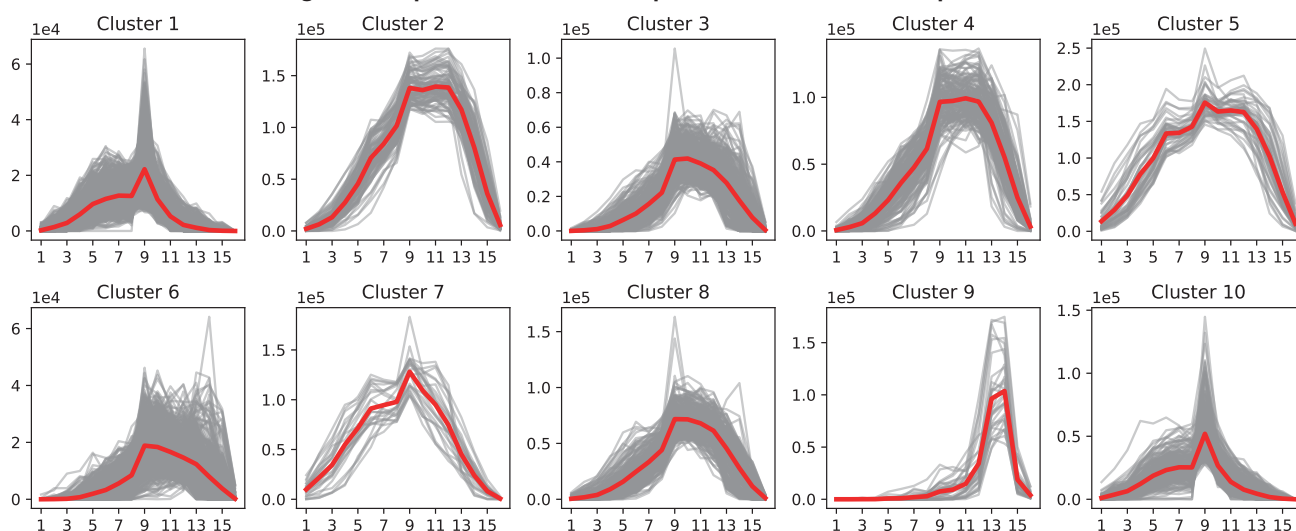


Fig. 5. Clusters identified by the *K*-means algorithm in the laboratory experiment. Gray lines show spectrum lines of the individual particles in each cluster. The red line is the average spectrum line in each cluster

Now consider the temporal distribution of particles in each cluster. Fig. 6 shows that particles in clusters 1 and 10 first appear when we inject *Betula* pollen into the detector (this moment is marked with a red vertical line) and then appear only in those periods when mixtures containing pollen of *Betula* were injected. Thus, one can identify the spectral profiles in clusters 1 and 10 as corresponding to *Betula*. Using the same reasoning, spectral profiles in clusters 2, 4, and 5 are identified with *Quercus* pollen. Surprisingly, particles from these clusters do not appear when the mixtures of *Betula* and *Quercus* are injected; however, they are observed when the mixture of all three pollen types is injected. The reason is not clear to us, and the only thing that we can note is that the mass content of *Quercus* pollen in the latter case was several times larger than in the previous mixtures. Considering the remaining clusters, one can note that cluster 7 has the first pronounced peak when *Phleum* pollen is injected and thus can be identified as this plant. In contrast, clusters 3, 6, and 9 appear at all times and even before the experiments started and can be attributed to background particles.

This laboratory experiment demonstrates that the proposed approach can be used to identify pollen types using spectrum profiles. The next step is to apply this method to the data from daily outdoor monitoring in the 2024 season.

Daily monitoring data

For the outdoor spectra measurements, we applied clustering with a large number of clusters ($K=70$) and obtained two groups of clusters. Particles in one group do not demonstrate any localized (in time) seasonal pattern. Their temporal distribution is similar to the distribution

of the total number of particles and is therefore non-informative. Particles in the second group have localized (in time) patterns and thus can be (potentially) identified with some specific pollen. Additionally, clusters whose temporal distribution had a similar pattern were merged into new superclusters. In fact, superclusters include spectra of similar shape but with different amplitudes. The final plots contain the temporal distribution of the merged clusters. Fig. 7 shows the temporal distributions of the particles in (some) superclusters, while Fig. 8 shows centers of the clusters that contribute to each supercluster.

Comparison of Fig. 7 with Fig. 2 does not reveal such clear correspondence as in the laboratory experiment. We can only propose some tentative interpretations. For example, cluster 6, spanning from mid-May to early June, looks consistent with the *Pinus* pollen. Cluster 3, mostly concentrated in the time interval from mid-April to mid-May, could be associated with *Betula* pollen. However, the peak in early April could indicate that *Acer* or *Corylus* pollen is mixed in this group. Cluster 2 is close in time with *Acer*. Cluster 5 is more prevalent during the summer and could contain grass pollen. Interestingly, the prominent peak in cluster 1 does not exhibit a correspondence with typical pollen in Fig. 2. In contrast, cluster 8 is present uniformly throughout all seasons, and we consider it background particles.

DISCUSSION

In this study, we examined the extent to which fluorescence spectra, measured by the Rapid E+ detector, can be linked to specific pollen types. We applied the *K*-means clustering algorithm to isolate groups of spectra with specific profiles and amplitudes within the whole set of

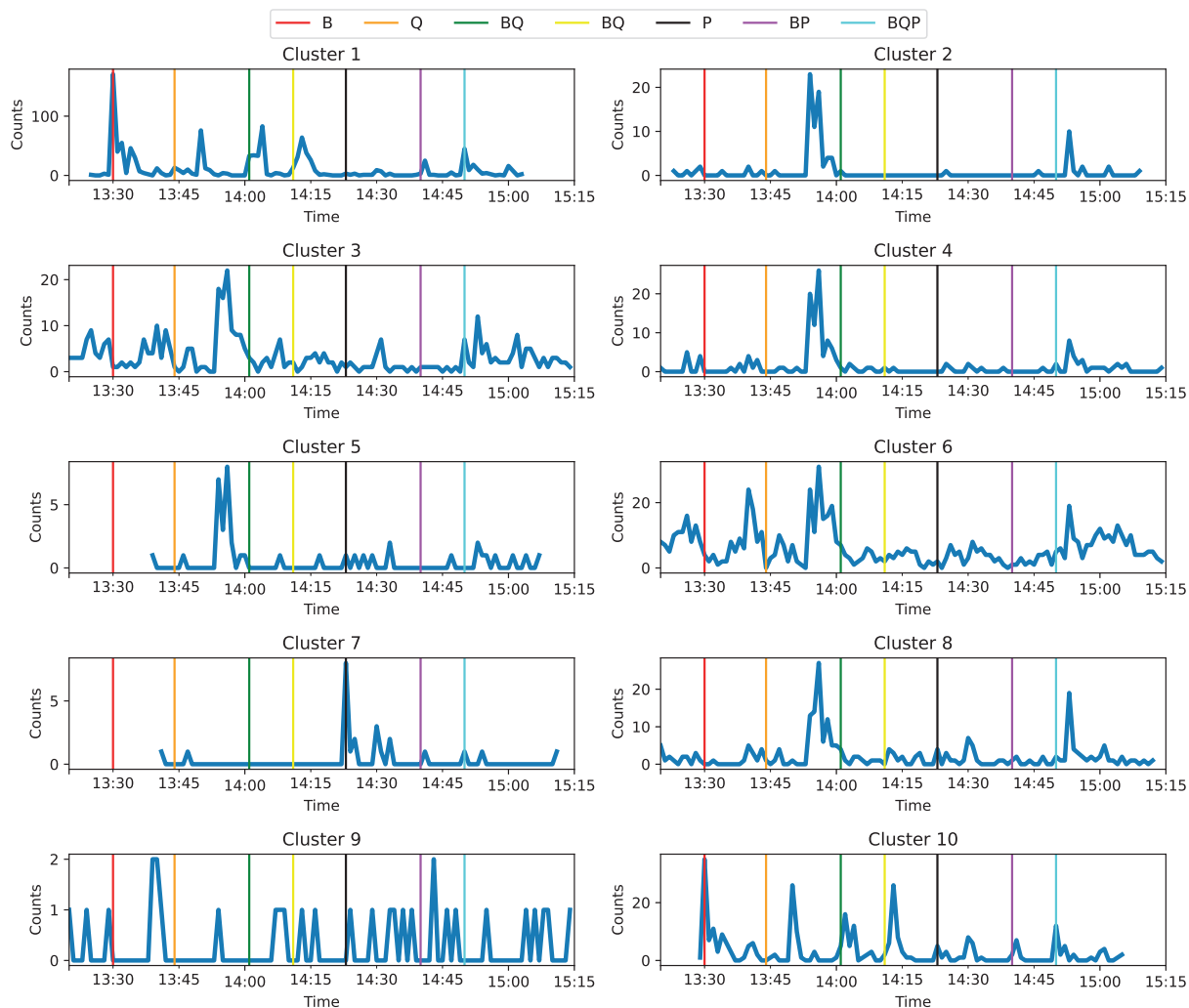


Fig. 6. Temporal distribution of the clusters identified by the *K*-means algorithm in the laboratory experiment

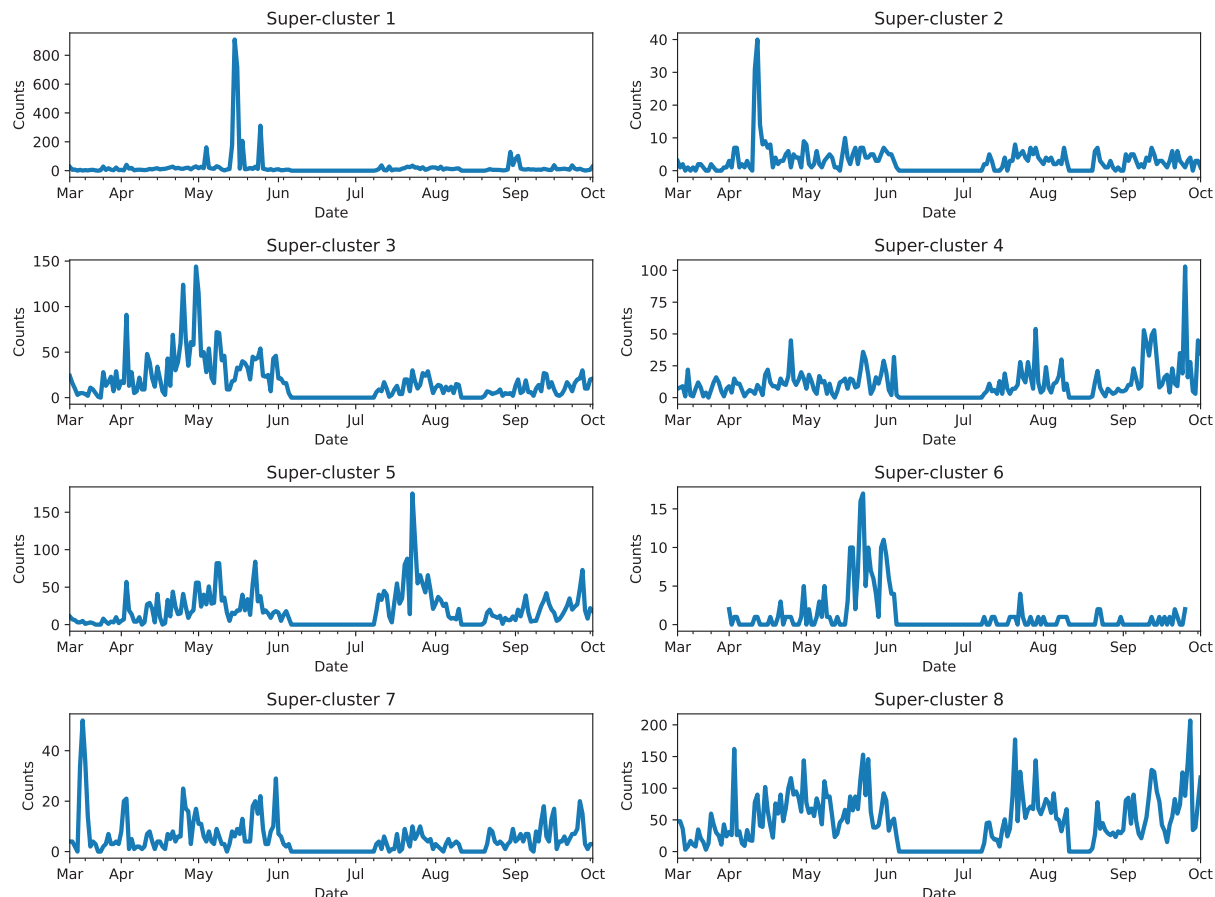


Fig. 7. Temporal distributions of particles in superclusters during the season 2024

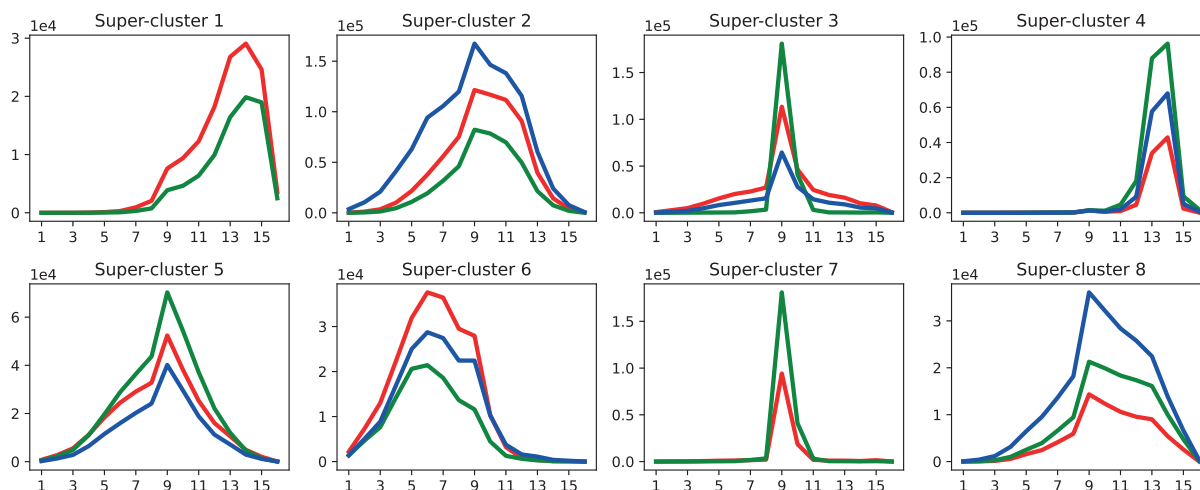


Fig. 8. Centers of the clusters that were merged to the superclusters. Each colored line represents the center of a separate cluster. The number of lines in each plot indicates the number of clusters merged into the super-cluster

measured spectra and analyzed the temporal distribution of the particles of the obtained groups (clusters). In laboratory conditions, when only a few pollen types are investigated and pollen is injected into the detector in portions in a clear form or as a known mixture, the proposed method yields quite straightforward associations. We observe that different pollen types have different spectrum profiles. In contrast, applying this approach to outdoor observation and comparing it with the volumetric data does not reveal as direct an association as one would like to see. We discuss some possible reasons below.

First, the clustering procedure is ambiguous. It depends on how the similarity (distance) between any two objects (see Blanco-Mallo, 2023, for further discussion) is measured, on the particular algorithm of clustering (K -means is probably the simplest but not unique one), and on the specific parameters of the particular algorithm (in the case of K -means, it depends on the number of clusters, initial position of cluster centers, and a number of more finer details).

In this study, we used the simplest Euclidean distance metric (sum of the squared differences between the corresponding components of the two vectors). Other distance metrics require modification of the K -means clustering algorithm itself (see, e.g., Kaufman & Rousseeuw, 1990). Actually, various clustering algorithms and various metrics were investigated, but qualitatively, the results appear similar.

The clustering results also depend on data preprocessing. For example, data normalization could help join spectra with similar shapes but different amplitudes into the same cluster. However, in fact this process often leads to joining in the same cluster spectra with different shapes, since it becomes more difficult to distinguish data by shape alone, rather than by shape and amplitude. For simplicity, we did not use any data preprocessing.

Instead, it turned out to be more practical to isolate a large number of clusters (much larger than the potential number of expected pollen types) and then join clusters that yield similar temporal distribution into superclusters (see, e.g., Xu et al., 2016, for possible estimates of the optimal number of clusters). In this research, we created superclusters manually based on visual analysis, but this step can also be automated using, say, clustering the time series.

Another thing to discuss is the correspondence of the clusters obtained in the laboratory experiment and during outdoor monitoring. Pollen used in the laboratory experiment is dry, while in outdoor monitoring, a mixture of dry and hydrated pollen may be observed. We do not know how the degree of hydration affects the fluorescence spectrum, so we leave it out of this research.

It should also be noted that outdoor measurements contain spectra of a much broader set of particle types than is reported in standard monitoring. In particular, we observe prominent clusters that are very localized in time but do not correspond to any of the pollen types reported in standard monitoring.

Finally, we used only a small part of the measurements provided by the automatic detector. It looks more than reasonable that finer separation of pollen types requires a combination of measured parameters. Furthermore, the known mass ratios of the pollen types used in laboratory experiments could be used in the future to estimate model accuracy in more detail.

CONCLUSIONS

In this work, we proposed a method for identification of pollen types using their fluorescence spectra measured by the automatic atmospheric particle detector Rapid-E+. The method is based on clustering of all fluorescence spectra measured by the detector and comparison of temporal patterns of occurrence of particles in each cluster with temporal patterns of occurrence of specific pollen types measured by the standard volumetric method. In a set of laboratory and outdoor experiments, it was demonstrated that fluorescence spectra are clustered into a set of groups that yield different distributions in time and that at least some of these groups are associated with specific pollen types. The obtained association can be used in the future to create an automatic pollen identification system. However, fluorescence data alone are insufficient for fine differentiation of all pollen types, and in fact, much larger groups representing mixtures of different pollen types are identified. At the same time, among these larger groups we observe those that are not identified by volumetric monitoring, and understanding the source of these particles is a matter of further research. ■

REFERENCES

- Akdis C. A., Hellings P. W., Agache I. (Eds.) (2015). European Academy of Allergy and Clinical Immunology. Global atlas of allergic rhinitis and chronic rhinosinusitis, EAACI, Zürich.
- An T., Liang Z., Chen Z., Li G. (2024). Recent progress in online detection methods of bioaerosols. *Fundamental Research*, 4 (3), DOI: 10.1016/j.fmre.2023.05.012.
- Bishop, C. M. (2007). *Pattern Recognition and Machine Learning (Information Science and Statistics)*, Springer.
- Blanco-Mallo E., Morán-Fernández L., Remeseiro B., Bolón-Canedo V. (2023). Do all roads lead to Rome? Studying distance measures in the context of machine learning. *Pattern Recognition*, 141, DOI: 10.1016/j.patcog.2023.109646.
- Boldeanu M., Burileanu C., Cucu H., Luminita Marmureanu L. (2022). Pollen classification using classical ML algorithms on fluorescence and scattering data. *U.P.B. Sci. Bull., Series C*, 84 (4).
- Brdar S., Panić M., Matavulj P. et al. (2023). Explainable AI for unveiling deep learning pollen classification model based on fusion of scattered light patterns and fluorescence spectroscopy. *Sci Rep* 13, 3205, DOI: 10.1038/s41598-023-30064-6.
- Buters J. T., Antunes C., Galveias A. et al. (2018). Pollen and spore monitoring in the world. *Clinical and translational allergy*, 8, 1-5. DOI:10.1186/s13601-018-0197-8
- Crouzy B., Stella M., Konzelmann T., Calpini B., Clot B. (2016). All-optical automatic pollen identification: Towards an operational system. *Atmospheric Environment*, 140, DOI: 10.1016/j.atmosenv.2016.05.062.
- D'Amato G. (2000). Urban air pollution and plant-derived respiratory allergy. *Clin. Exp. Allergy*, 30, 628–636. DOI: 10.1046/j.1365-2222.2000.00798.x.
- D'Amato, G., Vitale C., Sanduzzi A., Molino A., Vatrella, A., D'Amato M. (2017). Allergenic pollen and pollen allergy in Europe. *Allergy and allergen immunotherapy*, 287-306. DOI:10.1111/j.1398-9995.2007.01393.x.
- Daunys G., Šukienė L., Vaitkevičius L. et al. (2021). Clustering approach for the analysis of the fluorescent bioaerosol collected by an automatic detector. *PLoS One*, 16 (3), DOI: 10.1371/journal.pone.0247284.
- Dykewicz M. S., Hamilos D. L. (2010). Rhinitis and sinusitis. *Journal of Allergy and Clinical Immunology*, 125 (2), 103-115, DOI: 10.1016/j.jaci.2009.12.989.
- Erb, S., Graf, E., Zeder, Y., Lionetti, S., Berne, A., Clot, B., Lieberherr, G., Tummon, F., Wullschlegler, P., and Crouzy, B. (2024). Real-time pollen identification using holographic imaging and fluorescence measurements. *Atmos. Meas. Tech.*, 17, 441–451, DOI: 10.5194/amt-17-441-2024, 2024.
- Fröhlich-Nowoisky J., Kampf C. J., Weber B. et al. (2016). Bioaerosols in the Earth system: Climate, health, and ecosystem interactions. *Atmospheric Research*, 182, 346-376, DOI: 10.1016/j.atmosres.2016.07.018
- Galán C., Smith M., Thibaudon M. et al. (2014). Pollen monitoring: Minimum requirements and reproducibility of analysis. *Aerobiologia*, 30 (4), 385–395. DOI: 10.1007/s10453-014-9335-5
- Hirst J. M. (1952). An automatic volumetric spore trap. *The Annals of Applied Biology*, 39 (2), 257–265.
- Huffman J. A., Perring A. E., Savage N. J. et al. (2019). Real-time sensing of bioaerosols: Review and current perspectives. *Aerosol Science and Technology*, 54 (5), DOI: 10.1080/02786826.2019.1664724.
- Kabir E., Azzouz A., Raza N. et al. (2020). Recent Advances in Monitoring, Sampling, and Sensing Techniques for Bioaerosols in the Atmosphere. *ACS Sensors*, 5 (5), 1254-1267, DOI: 10.1021/acssensors.9b02585.
- Kaufman, L. and Rousseeuw, P.J. (1990). Partitioning Around Medoids (Program PAM). In *Finding Groups in Data* (eds L. Kaufman and P.J. Rousseeuw). DOI: 10.1002/9780470316801.ch2
- Matavulj P., Cristofori A., Cristofolini F., Gottardini E., Brdar S., Sikoparija B. (2022). Integration of reference data from different Rapid-E devices supports automatic pollen detection in more locations. *Science of The Total Environment*, 851 (2), DOI: 10.1016/j.scitotenv.2022.158234.
- Matavulj P., Jelic S., Severdija D., et al. (2025). Domain adaptation for improving automatic airborne pollen classification with expert-verified measurements. *Appl Intell* 55, 430, DOI: 10.1007/s10489-024-06021-9.
- Maya-Manzano J. M., Smith M., Markey E., Hourihane Clancy J., Sodeau J., O'Connor D. J. (2020). Recent developments in monitoring and modelling airborne pollen, a review. *Grana*, 60 (1), 1–19. DOI: 10.1080/00173134.2020.1769176.
- Oteros J., Buters J., Laven G., Roseler S. et al. (2017). Errors in determining the flow rate of Hirst-type pollen traps. *Aerobiologia*, 33, 201–210. DOI: 10.1007/s10453-016-9467-x, 2017.
- Šaulienė I., Šukienė L., Daunys G. et al. (2019). Automatic pollen recognition with the Rapid-E particle counter: the first-level procedure, experience and next steps. *Atmospheric Measurement Techniques*, 12, DOI: 10.5194/amt-12-3435-2019.
- Sikoparija B., Galán C., Smith M. et al. (2017). Pollen-monitoring: between analyst proficiency testing. *Aerobiologia*, 33, 191–199. DOI:10.1007/s10453-016-9461-3
- Šikoparija B., Matavulj P., Mimić G., Smith M., Grewling L., Podračanin Z. (2022). Real-time automatic detection of starch particles in ambient air. *Agricultural and Forest Meteorology*, 323, DOI: 10.1016/j.agrformet.2022.109034.
- Sofiev M., Bergman K.-C. (Eds.) (2012). *Allergenic Pollen: A Review of the Production, Release, Distribution and Health Impacts*. Springer.
- Swanson, B. E., Huffman, J. A. (2020). Pollen clustering strategies using a newly developed single-particle fluorescence spectrometer. *Aerosol Science and Technology*, 54 (4), 426–445, DOI: 10.1080/02786826.2019.1711357.
- Valenta R., Vrtala S., Ebner C., Kraft D., Scheiner O. (1992). Diagnosis of grass pollen allergy with recombinant timothy grass (*Phleum pratense*) pollen allergens. *Int. Arch. Allergy Immunol.*, 97, 287–294, DOI: 10.1159/000236135.
- Xu S., Qiao X., Zhang Y., Xue C., Li L. (2016). Reviews on Determining the Number of Clusters. *Applied Mathematics & Information Sciences*, 10, 1493-1512, DOI: 10.18576/amis/100428.